compartmentalization of components within the cell, and with temporal profiles of activation, to obtain a more comprehensive picture of the functional organization of a cell. Still, distance in chemical space (i.e., number of links between two distal nodes) is likely to be a major determinant of information processing that regulates phenotypic behavior.

The maps for individual ligands or cellular machines show distinct patterns of motifs. Combinations of ligands will likely produce many more patterns of connectivity. Thus, a cellular system may not be a single network but rather an ensemble of network configurations that are evoked by the stimuli-induced activation of various parts of the system. Identifying these network configurations and the functions they evoke is likely to provide more complete descriptions of how molecular interactions lead to cellular choices between homeostasis and plasticity.

References and Notes

1. J. D. Jordan, E. M. Landau, R. Iyengar, *Cell* **103**, 193 (2000).
2. U. S. Bhalla, R. Iyengar, *Science* **283**, 381 (1999).
3. U. S. Bhalla, P. T. Ram, R. Iyengar, *Science* **297**, 1018 (2002).
4. R. Iyengar, *Science* **271**, 461 (1996).
5. R. D. Blitzer *et al.*, *Science* **280**, 1940 (1998).
6. G. Lahav *et al.*, *Nat. Genet.* **36**, 147 (2004).
7. D. Angeli, J. E. Ferrell, E. D. Sontag, *Proc. Natl. Acad. Sci. U.S.A.* **101**, 1822 (2004).
8. S. Mangan, A. Zaslaver, U. Alon, *J. Mol. Biol.* **334**, 197 (2003).
9. S. Mangan, U. Alon, *Proc. Natl. Acad. Sci. U.S.A.* **100**, 11980 (2003).
10. D. J. Watts, S. H. Strogatz, *Nature* **393**, 440 (1998).
11. L. A. Amaral *et al.*, *Proc. Natl. Acad. Sci. U.S.A.* **97**, 11149 (2000).
12. A. L. Barabasi, R. Albert, *Science* **286**, 509 (1999).
13. T. V. Bliss, G. L. Collingridge, *Nature* **361**, 31 (1993).
14. S. A. Siegelbaum, E. R. Kandel, *Curr. Opin. Neurobiol.* **1**, 113 (1991).
15. Materials and methods are available as supporting material on *Science* Online.
16. O. Hvalby *et al.*, *Experientia* **43**, 599 (1987).
17. H. Katsuki, Y. Izumi, C. F. Zorumski, *J. Neurophysiol.* **77**, 3013 (1997).
18. H. Kang, E. M. Schuman, *Science* **267**, 1658 (1995).
19. N. Kashtan, S. Itzkovitz, R. Milo, U. Alon, *Bioinformatics* **20**, 1746 (2004).
20. P. V. Nguyen, T. Abel, E. R. Kandel, *Science* **265**, 1104 (1994).
21. R. Bourtchuladze *et al.*, *Cell* **79**, 59 (1994).
22. C. Pittenger, Y. Y. Huang, R. F. Paletzki *et al.*, *Neuron* **34**, 447 (2002).
23. G. Caldarelli *et al.*, *European Physical Journal B.* **38**, 183 (2004).

24. This research is supported by GM-54508 and GM-072853 from NIH and by an Advanced Research Center grant from the New York State Office of Science and Technology. A.M. is supported by Pharmacological Sciences Training grant GM-62754. S.N. is the recipient of an individual predoctoral National Research Service Award (GM-65065). R.D.B. is supported by National Institute on Drug Abuse grant DA15863. We thank B. Obrink, H. Dohlman, N. Hao, and J. Lisman for comments on the manuscript, M. Diverse-Pierluissi for help in identifying components of the secretory machine, S. Purushothaman for implementing the grid-coefficient function, and G. Kossinets (D. Watts laboratory, Columbia University, NY) for help with the initial analysis. Author contributions are described in the Supporting Online Material.

Supporting Online Material

www.sciencemag.org/cgi/content/full/309/5737/1078/DC1
Materials and Methods
SOM Text
Figs. S1 to S11
Tables S1 to S3
References

20 December 2004; accepted 7 July 2005
10.1126/science.1108876

Containing Pandemic Influenza at the Source

Ira M. Longini Jr.,[1]* Azhar Nizam,[1] Shufu Xu,[1] Kumnuan Ungchusak,[2] Wanna Hanshaoworakul,[2] Derek A. T. Cummings,[3] M. Elizabeth Halloran[1]

Highly pathogenic avian influenza A (subtype H5N1) is threatening to cause a human pandemic of potentially devastating proportions. We used a stochastic influenza simulation model for rural Southeast Asia to investigate the effectiveness of targeted antiviral prophylaxis, quarantine, and pre-vaccination in containing an emerging influenza strain at the source. If the basic reproductive number (R_0) was below 1.60, our simulations showed that a prepared response with targeted antivirals would have a high probability of containing the disease. In that case, an antiviral agent stockpile on the order of 100,000 to 1 million courses for treatment and prophylaxis would be sufficient. If pre-vaccination occurred, then targeted antiviral prophylaxis could be effective for containing strains with an R_0 as high as 2.1. Combinations of targeted antiviral prophylaxis, pre-vaccination, and quarantine could contain strains with an R_0 as high as 2.4.

The world may be on the brink of an influenza pandemic (*1–4*). Avian influenza A (subtype H5N1) is causing widespread outbreaks among poultry in Southeast (SE) Asia, with sporadic transmission from birds to humans (*5*) and limited probable human-to-human transmission (*6*). Should an avian virus reassort with a human virus, such as influenza A subtype H3N2, within a dually infected human host or reassort in a nonhuman mammalian species, or if mutation of the virus occurs, the resulting new variant could be capable of sustained human-to-human transmission. The outbreak among humans would then spread worldwide via the global transportation network more rapidly than adequate supplies of vaccine matched to the new variant could be manufactured and distributed (*1*, *7*). The pressing public health questions are whether and how we can contain the spread of an emerging strain at the source or at least slow the initial spread to give time for vaccine development. We used a discrete-time stochastic simulation model of influenza spread within a structured geographically distributed population of 500,000 people in SE Asia to compare the effectiveness of various intervention strategies against a new strain of influenza. Here we examine the effectiveness of the targeted use of influenza antiviral agents (*8–12*), quarantine, and pre-vaccination with a poorly matched, low-efficacy vaccine in containing the spread of the disease at the source.

We used information about rural SE Asia (*13, 14*) to construct the model population. Our goal was to represent the contact connectivity of a typical rural SE Asian population. The model population of 500,000 people was distributed across a space of 5625 km^2, yielding a density of 89/km^2, which is approximately the population density of rural SE Asia (*13*). The 500,000 people were partitioned into 36 geographic localities. This model is an extension of a model used to simulate interventions against pandemic influenza in the United States (*12*).

The model [see the supporting online material (SOM) for details] represents the number of close and casual contacts that a typical person makes in the course of a day. The age and household size distributions of the population are based on the Thai 2000 census (*13*). Many of the mixing group sizes and distributions are based on a social network study of the Nang Rong District in rural Thailand (*14*). We constructed the social network for contacts sufficient to transmit influenza as a large set of connected mixing groups. The close contact groups consist of households, household clusters, preschool groups, schools, and workplaces; and the casual contact groups consist of other social settings (such as markets, shops, and temples) and a single regional 40-bed hospital. All people can

[1]Department of Biostatistics, The Rollins School of Public Health, Emory University, 1518 Clifton Road, N.E., Atlanta, GA 30322, USA. [2]Ministry of Public Health, Nonthaburi, Thailand. [3]Department of International Health, The Bloomberg School of Public Health, Johns Hopkins University, Baltimore, MD, USA.

*To whom correspondence should be addressed. E-mail: longini@sph.emory.edu

mix in their households and within clusters of households, whereas children mix in preschool groups or schools according to their age and the probability that they are still in school. Children are assigned to schools across the geographic space according to the Nang Rong study. Adults mix in workplaces according to a distance function that distributes them across the geographic space informed by the Nang Rong study and national migration statistics (*15*, *16*). One concern for containment is that infected people might leave the modeled 500,000-person rural area. We estimate that the daily probability that a person will leave (escape) the area is on the order of 10^{-3} (*15*). The population structure and the resulting social network graphs and statistics are given in the SOM.

The natural history of influenza (Fig. 1A) has been relatively invariant over the past two pandemics and during the interpandemic period since 1968 (*12*, *17*–*20*). Calibration of the model requires information about both the relative and absolute magnitudes of the age-specific illness attack rates. Because of uncertainty about the relative age-specific illness attack rates for a future influenza pandemic in SE Asia, we calibrated the epidemic to a pattern that falls between two extremes. At one extreme, children would have a much higher illness attack rate than adults, the pattern observed during the 1957–1958 A (subtype H2N2) Asian influenza pandemic in the United States (*17*, *21*, *22*). At the other extreme, all age groups would have roughly the same illness attack rates, the pattern observed during the 1968–1969 A (H3N2) Hong Kong influenza pandemic in the United States (*17*, *22*–*24*). The pattern for interpandemic influenza in SE Asia appears to be more like the A (H2N2) pattern (*25*). We used the pattern shown in Fig. 1B.

The magnitude of the illness attack rates will depend on the unknown transmissibility of the new strain. The overall illness attack rate for the past Asian and Hong Kong pandemics was about 33% in the first wave. We calibrated the model with a target overall illness attack rate of 33%, corresponding to a basic reproductive number (R_0) (the average number of secondary infections caused by a single typical infectious individual in a completely susceptible population) of 1.4 (see the SOM). By varying the per-contact probability of infection in the model, we alter the R_0. Figure 1B shows the age-specific attack rates at R_0 values ranging from 1.1 to 2.4. For calibration to historical attack rates, influenza was introduced by randomly assigning 12 initial infectives. We simulated the emergence of a new influenza strain by introducing a single randomly assigned infective.

Intervention is triggered by the first case (that is, symptomatic infection), with a delay of 7, 14, or 21 days to implementation. This delay can be interpreted as a delay in recognition of illness, a delay in implementation of intervention, initiation of transmission by more than one initial infection, or a combination of these three factors. A sensitivity analysis considers delays up to 56 days (fig. S14). Once intervention begins, intervention in additional localities is implemented 1 day after the first case in the affected locality.

Targeted antiviral prophylaxis (TAP) is carried out by treating identified index cases (the first symptomatic illness in a mixing group) and offering prophylaxis only to the contacts of these index cases in predefined close contact groups (*12*); namely, households, neighborhood clusters, preschool groups, schools, and workplaces. Index cases are therapeutically treated the day after the onset of illness, and prophylaxis of contacts begins at the same time, both being given a single course of oseltamivir. A susceptible individual may receive subsequent courses if exposed to further index cases. We assume that a certain percent, varied in a sensitivity analysis, of household (preschool) index cases could be ascertained and that all their other household (preschool) members would receive prophylaxis (fig. S11). For index cases in a school or workplace, only

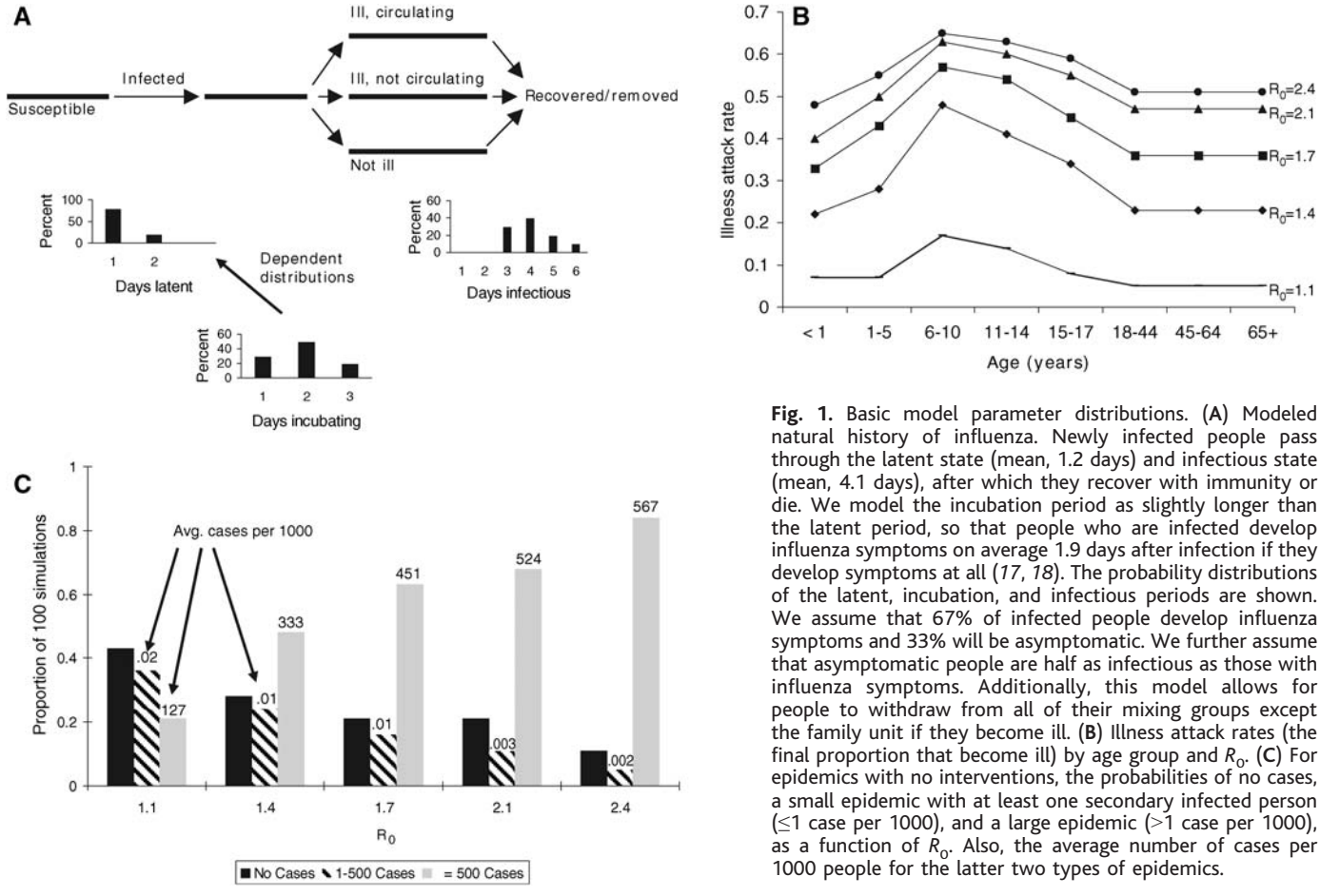

Fig. 1. Basic model parameter distributions. (**A**) Modeled natural history of influenza. Newly infected people pass through the latent state (mean, 1.2 days) and infectious state (mean, 4.1 days), after which they recover with immunity or die. We model the incubation period as slightly longer than the latent period, so that people who are infected develop influenza symptoms on average 1.9 days after infection if they develop symptoms at all (*17*, *18*). The probability distributions of the latent, incubation, and infectious periods are shown. We assume that 67% of infected people develop influenza symptoms and 33% will be asymptomatic. We further assume that asymptomatic people are half as infectious as those with influenza symptoms. Additionally, this model allows for people to withdraw from all of their mixing groups except the family unit if they become ill. (**B**) Illness attack rates (the final proportion that become ill) by age group and R_0. (**C**) For epidemics with no interventions, the probabilities of no cases, a small epidemic with at least one secondary infected person (≤1 case per 1000), and a large epidemic (>1 case per 1000), as a function of R_0. Also, the average number of cases per 1000 people for the latter two types of epidemics.

a certain percent of the people in that mixing group would receive prophylaxis. We used current estimates of the antiviral efficacy (AVE) of oseltamivir (*26*–*29*) (see the SOM).

The primary difficulty in TAP would be the identification of index cases. Because TAP is aimed at predefined close contact groups, the identification of potential TAP recipients would be less difficult than in classical contact tracing. An alternative and less resource-intensive strategy would be geographically targeted antiviral prophylaxis (GTAP), also known as ring prophylaxis. In this strategy, once an influenza case is identified in a locality, then a percentage, varied in a sensitivity analysis (fig. S12), of people in an entire locality are given one course of oseltamivir.

Household quarantine, like GTAP, is implemented within localities. The first case in a locality triggers a quarantine policy. Every case and a certain percentage of susceptible people restrict their movement to within their household and their neighborhood cluster. Because quarantined people would have more contact with their household and neighborhood contacts, the contact probabilities within households and household clusters are doubled for quarantined people.

A human influenza A (H5N1) vaccine is currently being tested (*7*) and may be available, but could be poorly matched to the emerging strain and thus be of low efficacy. For the model scenarios that use vaccination, we assume that pre-vaccination takes place long enough before the pandemic that vaccinated people can develop immunity. We assume a low vaccine efficacy for susceptibility (VE_S) (*30*) of 0.30 and a vaccine efficacy for infectiousness (VE_I) of 0.50. We carried out a sensitivity analysis on VE_I (fig. S19).

We consider an epidemic to be contained if there are fewer than 500 cases in the 500,000-person community (≤1 per 1000). The containment proportion is the proportion of simulations in which the attack rate is ≤1 per 1000. Another measure of how well we have contained the epidemic is the number of infected people who travel out of the 500,000-person community over the course of the epidemic. If this number is very low or even zero, we have effectively contained spread at the source. The number of cases per 1000 people in the population is another measure of success of the intervention.

Given an initial person infected with the newly emergent influenza strain, there are three possible outcomes: (i) no further people are infected; (ii) there is a small epidemic, between 1 and 500 total cases (≤1 per 1000); or (iii) there is a large epidemic (>1 case per 1000 people). The relative probabilities of these three outcomes as well as the average size of a large epidemic vary with R_0 (Fig. 1C).

Figure 2A shows a typical realization of a large epidemic due to a single initial infective at R_0 = 1.4, with no intervention, as well as the average times for intervention initiation. On average, the first symptomatic case appeared 4 days after the initial infection, with intervention initiation times on average 11, 18, or 25 days after the initial infection. Figure 2B shows a typical realization of an epidemic contained with 90% GTAP. Movies 1 to 3 in the SOM show the geographic spread of the epidemic with and without intervention.

Figure 3 gives bar plots of the results for the different intervention strategies and values of R_0. Table 1 gives numbers for the results for R_0 values of 1.4 and 1.7. The measures of containment did not vary much if intervention was initiated 7, 14, or 21 days after the first case, so we give results just for the 14-day delay, followed by a sensitivity analysis of the effect of further delay (fig. S14). When R_0 = 1.1, just above threshold, all of the interventions work well. Both 80% TAP and 90% GTAP would be effective in containing pandemic influenza at the source if $R_0 \leq 1.4$. If $R_0 \geq 1.7$, then neither 80% TAP nor 90% GTAP is consistently effective in containing the epidemic, and 300,000 to 350,000 courses of oseltamivir would be needed. Thus, for these interventions singly, a containment threshold exists somewhere between R_0 = 1.4 and 1.7. Further sensitivity analysis shows that the containment threshold is roughly at R_0 = 1.6.

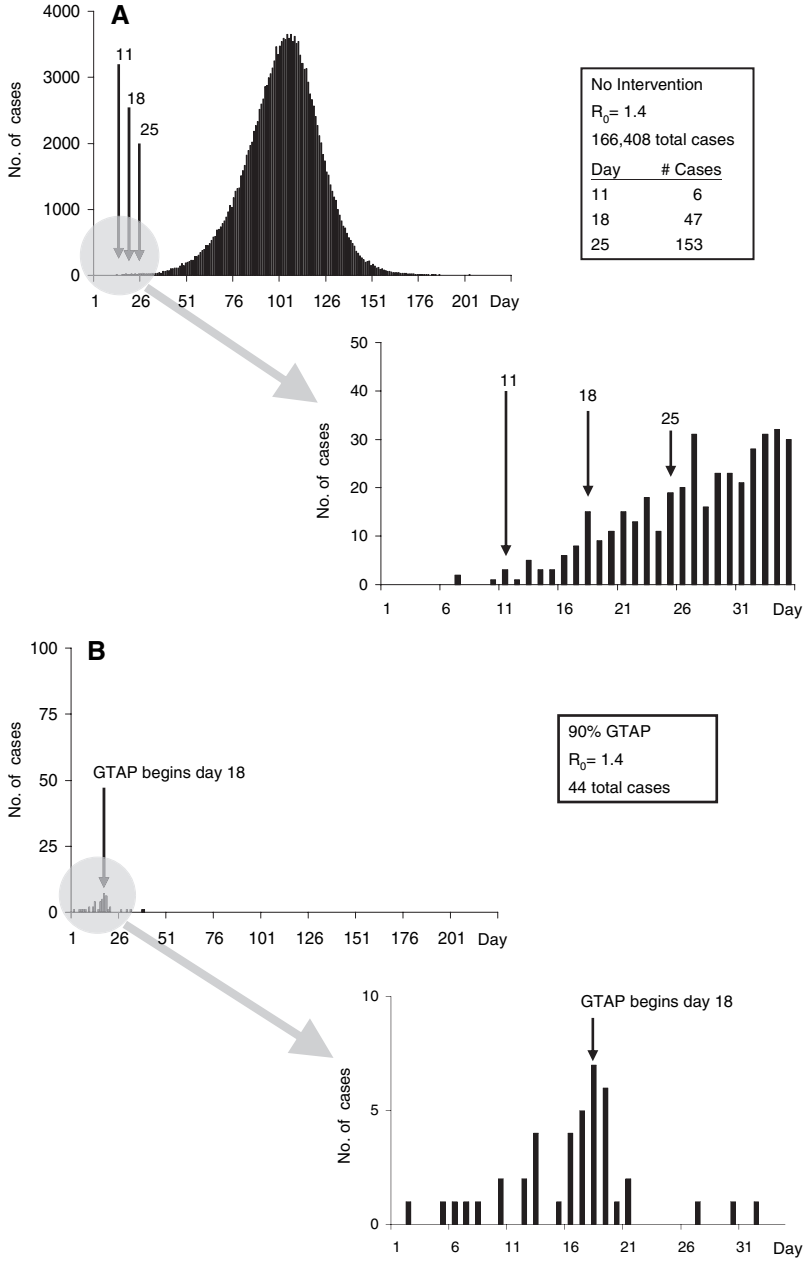

Fig. 2. Model stochastic realizations. (**A**) A typical stochastically simulated large influenza epidemic with no intervention and R_0 = 1.4. Also shown are the main intervention initiation times considered and the number of cases at those intervention times. (**B**) A typical stochastically simulated influenza epidemic that is contained using 90% GTAP initiated 14 days after the first case, when R_0 = 1.4.

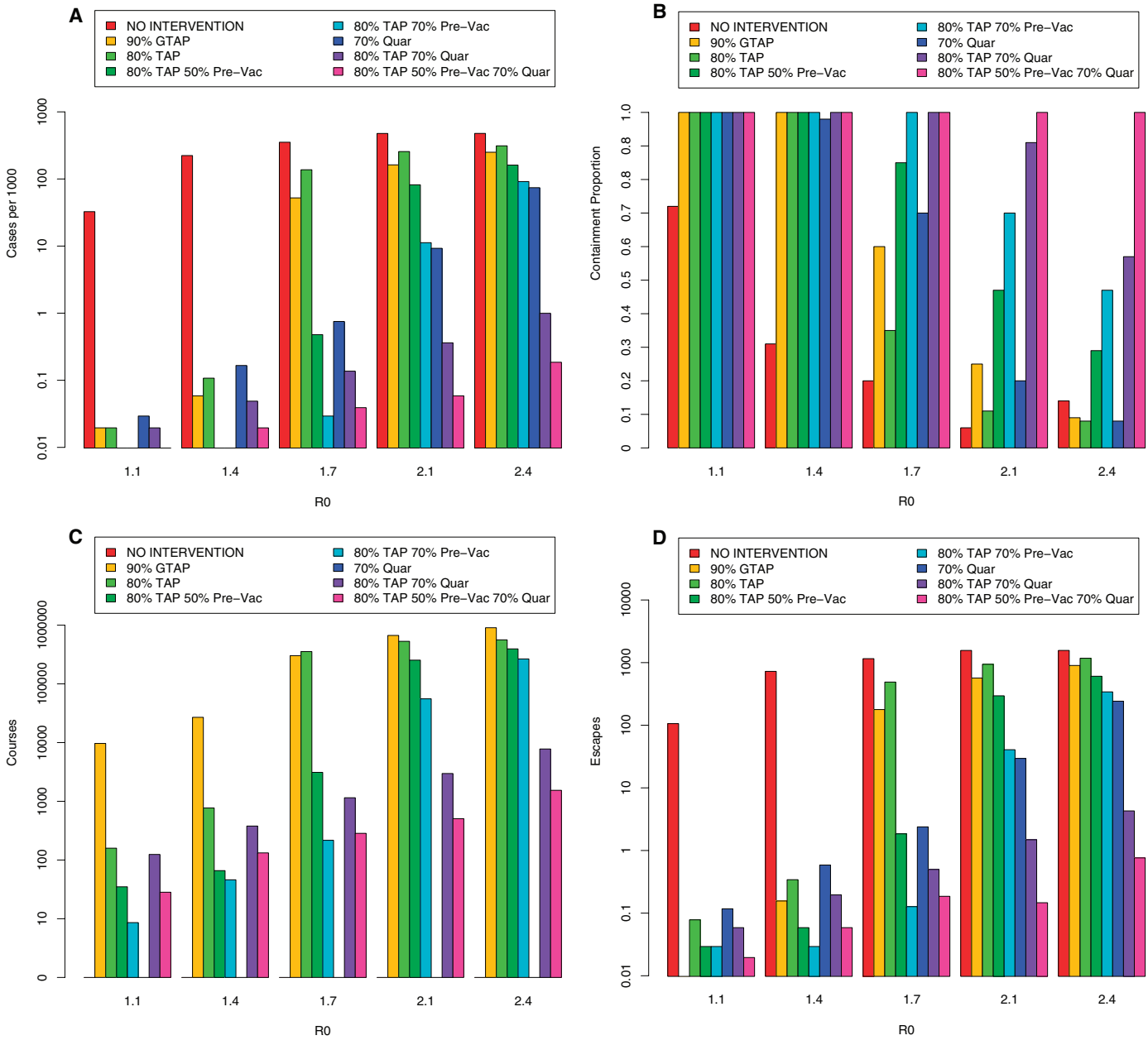

Fig. 3. The effectiveness of the different interventions as compared to no intervention started 14 days after the first case at different values of R_0. The interventions considered are 90% GTAP, 80% TAP, 80% TAP plus 50% pre-vaccination of the population (80% TAP 50% Pre-Vac), 80% TAP plus 70% pre-vaccination of the population (80% TAP 70% Pre-Vac), 70% household and household cluster quarantine (70% Quar), 80% TAP with 70% household and household cluster quarantine (80% TAP 70% Quar), and 80% TAP plus 50% pre-vaccination of the population with 70% household and household cluster quarantine (80% TAP 50% Pre-Vac 70% Quar). (**A**) Average number of cases per 1000 people with no intervention and with different interventions. (**B**) Average containment proportion defined as the proportion of epidemics with one or more secondary cases that had 500 or fewer cases in the population of 500,000 (or $\leq$1 case per 1000). The "no intervention" entry gives the proportion of these epidemics that had 500 or fewer cases with no intervention in the population of 500,000 (or $\leq$1 case per 1000). (**C**) Average number of infected people leaving the 500,000-person population. Each day, the number of infected people who have not withdrawn to the home or are quarantined is multiplied by 10^{-3}, the probability that a person will travel outside of the 500,000-person area. (**D**) Average number of courses of oseltamivir used for the intervention.

Pre-vaccination of the population with a low-efficacy vaccine greatly enhances the effectiveness of TAP and GTAP, even with just 50% coverage. With pre-vaccination, both 80% TAP and 90% GTAP are effective at containing the epidemic when $R_0 = 1.7$, but not at higher levels of R_0. Pre-vaccination essentially lowers the reproductive number (*31*). Local household quarantine is effective at containing the epidemic if $R_0 \leq 2.1$ but is not as effective at $R_0 = 2.4$. However, a combination of 80% TAP plus quarantine is effective at an R_0 as high as 2.4, and adding pre-vaccination makes TAP plus quarantine even more effective.

We conducted a number of sensitivity analyses of the effectiveness of the different interventions at different levels of implementation and delay (figs. S11 to S18). We found that at $R_0 \leq 1.4$, either TAP or GTAP alone is effective only at the 70% level or higher. At higher values of R_0, household quarantine must reach the 70% level to be effective. In terms of timing of the intervention (fig. S14), 90% GTAP and 80% TAP become less effective when the intervention starts 28 days or more after the detection of the first symptomatic case, when there is an average of 85 cases already. Quarantine at the 70% level becomes less effective 42 days (average, 313 cases)

Table 1. Simulated mean cases, escapes, courses, and containment proportion for various interventions and no intervention in a typical rural population of 500,000 people in SE Asia.

Intervention	Cases per 1000		Escapes		Courses		Containment proportion	
	$R_0 = 1.4$	$R_0 = 1.7$	$R_0 = 1.4$	$R_0 = 1.7$	$R_0 = 1.4$	$R_0 = 1.7$	$R_0 = 1.4$	$R_0 = 1.7$
No intervention	211	384	686	1254	–	–	–	–
80% TAP	0.13	149	0.43	525	1,042	381,273	0.98	0.33
90% GTAP	0.28	54	1	187	54,834	325,431	0.95	0.59
80% TAP + 50% pre-vaccination	0.02	0.16	0.06	0.67	87	1,338	1.00	0.98
80% TAP + 70% pre-vaccination	0.01	0.04	0.08	0.12	67	269	1.00	1.00
70% quarantine	0.17	1	0.72	3	-	-	0.98	0.57
80% TAP + 70% quarantine	0.06	0.14	0.18	0.36	484	1,349	1.00	1.00
80% TAP + 70% quarantine + 50% pre-vaccination	0.02	0.03	0.06	0.17	91	275	1.00	1.00

after detection of the first case, even with the addition of TAP. All other interventions in combination with pre-vaccination would be fairly effective even 56 days (average, 894 cases) after the detection of the first case.

It may not be practical to get antiviral agents to exposed people within 1 day of the index case developing symptoms. We carried out a sensitivity analysis for delays in initiation of TAP in the close contact mixing groups ranging from 2 to 5 days after detection of an index case, with 80% TAP. With a delay of up to 2 days, substantial reduction in the number of cases is still achieved, but with delays of 3 to 5 days, there is less benefit (fig. S15). Sensitivity analysis on antiviral efficacy (figs. S16 to S18) shows that the effectiveness of TAP and GTAP is moderately sensitive to variation in AVE_S but not as much to variation in antiviral efficacy in preventing symptomatic disease if infected, AVE_D. Both AVE_S and AVE_I need to be 0.5 or higher for either TAP or GTAP to be effective. Sensitivity analysis on VE_I shows that the effectiveness of 80% TAP with 70% pre-vaccination is sensitive to variation in VE_I (fig. S19). However, even at a level of VE_I as low as 0.1 (fig. S19), the epidemic is still well contained.

We have shown that the targeted use of antiviral agents, if implemented within 21 days of the first case and if $R_0 \leq 1.4$, would have a high probability of success for containing an emergent influenza strain at the source in a rural SE Asian population. Such interventions would be effective for R_0 values as high as 1.7 in the presence of pre-vaccination with a low-efficacy vaccine. For higher values of R_0, localized household quarantine would have to be implemented, possibly in combination with targeted antiviral prophylaxis to contain the pandemic at the source. Although the R_0 of a future newly emergent influenza strain is unknown, previous estimates are 1.89 from the first epidemic of pandemic A (H3N2) in Hong Kong (*19*) and 2 to 3 for 1918 pandemic A (H1N1) in the United States (*32*). However, a newly emergent influenza strain may not yet be well adapted to humans and could have an $R_0 < 2$, and possibly just above 1. As the virus adapts to human-to-human transmission, there would probably be an incremental increase in R_0 with each transmission event (*33*). This makes early intervention especially important.

Based on the results here, the current World Health Organization stockpile of 120,000 treatment courses could possibly be sufficient to contain a pandemic if the stockpile were deployed at the source of the emerging strain within 2 to 3 weeks of detection. Given that early containment at the original source may fail or the emergent strain may appear simultaneously in several locations, up to 1 million courses could be needed to deal with the multiple outbreak foci. In addition, pre-vaccination of populations at risk for a newly emergent influenza strain would be prudent, even if the vaccine provided only moderate protection. Although the effectiveness of most interventions was fairly invariant to the timing of intervention initiation up to 21 days after the first case, delay much beyond that could allow the pandemic to spread unless pre-vaccination takes place.

These results are probabilistic and demonstrate considerable variability in the potential size of the epidemic in the absence of and in response to intervention (*34*). Public health officials need to keep this probabilistic characteristic of success in mind when planning and evaluating their response. We have developed a flexible mathematical model that can help determine the best intervention strategies for containing pandemic influenza at the source. Should a newly emergent influenza strain appear, the model could be quickly calibrated to data and intervention options at the source of the epidemic. Data should be provided from the field to estimate the value of R_0; the serial interval between cases; the distributions of the latent, incubation, and infectious periods; pathogenicity; case fatality ratios; and secondary spread within important mixing groups.

References and Notes

1. R. J. Webby, R. G. Webster, *Science* **302**, 1519 (2003).
2. M. Enserink, *Science* **306**, 2016 (2004).
3. K. Stohr, *N. Engl. J. Med.* **352**, 405 (2005).
4. A. S. Monto, *N. Engl. J. Med.* **352**, 323 (2005).
5. N. M. Ferguson, C. Fraser, C. A. Donnelly, A. C. Ghani, R. M. Anderson, *Science* **304**, 968 (2004).
6. K. Ungchusak *et al.*, *N. Engl. J. Med.* **352**, 333 (2005).
7. K. Stohr, M. Esveld, *Science* **306**, 2195 (2004).
8. F. G. Hayden, *Philos. Trans. R. Soc. London Ser. B* **356**, 1877 (2001).
9. R. G. Webster, *Science* **293**, 1773 (2001).
10. G. Laver, E. Garman, *Science* **293**, 1776 (2001).
11. A. S. Monto *et al.*, *JAMA* **282**, 31 (1999).
12. I. M. Longini, M. E. Halloran, A. Nizam, Y. Yang, *Am. J. Epidemiol.* **159**, 623 (2004).
13. National Statistical Office, *Population and Housing Census 2000* (available at www.nso.go.th, accessed 19 November 2004).
14. K. Faust, B. Entwisle, R. R. Rindfuss, S. J. Walsh, Y. Sawangdee, *Soc. Networks* **21**, 311 (1999).
15. P. Guest, A. Chamraathrithirong, K. Arhavanitkul, N. Piriyathamwong, *Asian Pacific Migrat. J.* **3**, 531 (1994).
16. A. Chamraathrithirong *et al.*, *National Migration Survey of Thailand* (Institute for Population and Social Research, Mahidol Univeristy, Bangkok, Thailand, 1995).
17. L. R. Elveback *et al.*, *Am. J. Epidemiol.* **103**, 152 (1976).
18. E. D. Kilbourne, *The Influenza Viruses and Influenza* (Academic Press, New York, 1975).
19. L. A. Rvachev, I. M. Longini, *Math. Biosci.* **75**, 3 (1985).
20. S. Cauchemez, F. Carrat, C. Viboud, A. J. Valleron, P. Y. Boëlle, *Stat. Med.* **23**, 3469 (2004).
21. W. S. Jordan, *Am. Rev. Res. Dis.* **83**, 29 (1961).
22. I. M. Longini, E. Ackerman, L. R. Elveback, *Math. Biosci.* **38**, 141 (1978).
23. L. E. Davis, G. C. Caldwell, R. E. Lynch, R. E. Bailey, *Am. J. Epidemiol.* **92**, 240 (1970).
24. R. G. Sharrar, *Bull. World Health Org.* **41**, 361 (1969).
25. K. A. Fitzner, S. M. McGhee, A. J. Hedley, K. F. Shortridge, *Hong Kong Med. J.* **5**, 87 (1999).
26. F. G. Hayden, F. Y. Aoki, in *Antimicrobial Therapy and Vaccines*, V. Yu, T. Meigan, S. Barriere, Eds. (Williams and Wilkins, Baltimore, MD, 1999), pp. 1344–1365.
27. F. G. Hayden *et al.*, *N. Engl. J. Med.* **343**, 1282 (2000).
28. R. Welliver *et al.*, *JAMA* **285**, 748 (2001).
29. Y. Yang, I. M. Longini, M. E. Halloran, *Design and Evaluation of Prophylactic Interventions Using Infectious Disease Incidence Data from Close Contact Groups* (Technical Report 04-09, Department of Biostatistics, Emory University, Atlanta, GA, 22 July 2004) (available at www.sph.emory.edu/bios/tech/).
30. M. E. Halloran, I. M. Longini, C. J. Struchiner, *Epidemiol. Rev. Vaccines* **21**, 73 (1999).
31. A. N. Hill, I. M. Longini, *Math. Biosci.* **181**, 85 (2003).
32. C. E. Mills, J. M. Robins, M. Lipsitch, *Nature* **432**, 904 (2004).
33. R. Antia, R. R. Regoes, J. C. Koella, C. T. Bergstrom, *Nature* **426**, 658 (2003).
34. M. E. Halloran, I. M. Longini, D. M. Cowart, A. Nizam, *Vaccine* **20**, 3254 (2002).

35. This work was supported by National Institute of General Medical Sciences MIDAS grant U01-GM070749 and National Institute of Allergy and Infectious Diseases grant R01-AI32042. The authors thank F. Hayden, K. Stöhr, P. Glezen, A. Monto, S. Dowell, and B. Schwartz for their helpful comments.

Supporting Online Material

www.sciencemag.org/cgi/content/full/1115717/DC1
SOM Text
Figs. S1 to S19
Tables S1 to S7
References
Movies S1 to S3

6 June 2005; accepted 14 July 2005
Published online 3 August 2005;
10.1126/science.1115717
Include this information when citing this paper.

Containing Pandemic Influenza at the Source

Ira M. Longini Jr., Azhar Nizam, Shufu Xu, Kumnuan Ungchusak, Wanna Hanshaoworakul, Derek A. T. Cummings and M. Elizabeth Halloran

Science **309** (5737), 1083-1087.
DOI: 10.1126/science.1115717originally published online August 3, 2005